



The ADP-Heptose Biosynthesis Enzyme GmhB is a Conserved Gram-Negative Bacteremia Fitness Factor

 Caitlyn L. Holmes,^{a,b} Sara N. Smith,^b Stephen J. Gurczynski,^b  Geoffrey B. Severin,^b Lavinia V. Unverdorben,^{a,b} Jay Vornhagen,^{a,b} Harry L. T. Mobley,^b  Michael A. Bachman^{a,b}

^aDepartment of Pathology, University of Michigan Medical School, Ann Arbor, Michigan, USA

^bDepartment of Microbiology and Immunology, University of Michigan Medical School, Ann Arbor, Michigan, USA

ABSTRACT *Klebsiella pneumoniae* is a leading cause of Gram-negative bacteremia, which is a major source of morbidity and mortality worldwide. Gram-negative bacteremia requires three major steps: primary site infection, dissemination to the blood, and bloodstream survival. Because *K. pneumoniae* is a leading cause of health care-associated pneumonia, the lung is a common primary infection site leading to secondary bacteremia. *K. pneumoniae* factors essential for lung fitness have been characterized, but those required for subsequent bloodstream infection are unclear. To identify *K. pneumoniae* genes associated with dissemination and bloodstream survival, we combined previously and newly analyzed insertion site sequencing (InSeq) data from a murine model of bacteremic pneumonia. This analysis revealed the gene *gmhB* as important for either dissemination from the lung or bloodstream survival. In *Escherichia coli*, GmhB is a partially redundant enzyme in the synthesis of ADP-heptose for the lipopolysaccharide (LPS) core. To characterize its function in *K. pneumoniae*, an isogenic knockout strain ($\Delta gmhB$) and complemented mutant were generated. During pneumonia, GmhB did not contribute to lung fitness and did not alter normal immune responses. However, GmhB enhanced bloodstream survival in a manner independent of serum susceptibility, specifically conveying resistance to spleen-mediated killing. In a tail-vein injection of murine bacteremia, GmhB was also required by *K. pneumoniae*, *E. coli*, and *Citrobacter freundii* for optimal fitness in the spleen and liver. Together, this study identifies GmhB as a conserved Gram-negative bacteremia fitness factor that acts through LPS-mediated mechanisms to enhance fitness in blood-filtering organs.

KEYWORDS *Citrobacter*, *Escherichia coli*, *Klebsiella*, bloodstream infections, gram-negative bacteria, lipopolysaccharide, pneumonia

Gram-negative bacteremia is a significant cause of global morbidity and mortality largely due to progression to sepsis, defined as life-threatening organ dysfunction resulting from a dysregulated host response to infection (1). Gram-negative pathogens underlie 43% of clinical bloodstream infections with a small number of species, including *Escherichia coli*, *Klebsiella pneumoniae*, *Citrobacter freundii*, and *Serratia marcescens*, contributing to the majority of cases (2, 3). Of these species, *K. pneumoniae* is the second most common species causing Gram-negative bacteremia and the third most prevalent cause of all bloodstream infections (2). Although *K. pneumoniae* can be a commensal species (4, 5), it is also an opportunistic pathogen. This is especially relevant in health care-associated infections where *K. pneumoniae* is a leading source of disease (6). The Centers for Disease Control and Prevention have repeatedly classified carbapenem-resistant *Enterobacterales*, including *K. pneumoniae*, as an urgent public health threat due to antibiotic resistance (7, 8). Bacteremia from antibiotic-resistant

Editor Nancy E. Freitag, University of Illinois at Chicago

Copyright © 2022 Holmes et al. This is an open-access article distributed under the terms of the [Creative Commons Attribution 4.0 International license](https://creativecommons.org/licenses/by/4.0/).

Address correspondence to Michael A. Bachman, mikebach@med.umich.edu.

The authors declare no conflict of interest.

Received 7 June 2022

Accepted 12 June 2022

Published 28 June 2022

K. pneumoniae can be extremely difficult to treat and is associated with a high mortality rate.

The pathogenesis of Gram-negative bacteremia involves three main phases: primary site infection, dissemination, and bloodstream survival (3). First, bacteria must invade primary sites of infection or colonization and evade local host responses. Second, pathogens disseminate across host barriers to gain bloodstream access, a process that varies based on the initial site. Navigation across barriers may include strategies to invade or disrupt site-specific epithelial cells, endothelial cells, and cellular junctions. Third, bacteria must exercise metabolic flexibility and resist host defenses in the bloodstream to adapt in a new environment. In circulation, bacteria passage through blood filtering organs, like the spleen and liver, which may act as additional sites of infection from which dissemination can occur. Defects at initial sites do not always predict fitness at secondary sites (9, 10), and apparent lack of fitness at secondary sites may be confounded by defects at the initial site. Therefore, observed overlap between primary site and bloodstream fitness genes highlight the necessity to probe phases of bacteremia separately to correctly define stages relevant to pathogenesis (3). By carefully defining the bacterial factors required for each phase of bacteremia, we may identify therapeutic targets for interventions that prevent progression to bacteremia or treat it more effectively once it has occurred.

K. pneumoniae bacteremia is often secondary to pneumonia (6) and fitness factors for primary site infection in the lung have been extensively investigated. Capsular polysaccharide, siderophores, and synthesis of branched-chain amino acids (11–13) are required for lung fitness. Additionally, the citrate (Si)-synthase GltA, and the acetyltransferase Atf3, are required (9, 10), highlighting the broad range of factors contributing to lung initial site fitness. Some fitness factors in the lung are also likely to be important in the bloodstream. Capsular polysaccharide is required to resist human serum complement, and siderophores are important for both dissemination from the lung and growth in human serum (12). However, factors that act specifically at the stages of dissemination and bloodstream survival are unclear. Genes necessary for serum resistance have been described *in vitro* and include cell wall integrity proteins, and multiple metabolic pathways (14, 15), but factors that resist host responses during bacteremia and allow growth within blood-filtering organs is unknown.

In the bloodstream, cell surface structures can defend bacteria from environmental threats like formation of the membrane attack complex or antimicrobial peptides. Of these, lipopolysaccharide (LPS) is a defining cellular envelope structure of Gram-negative species that governs many environmental interactions and aids in resistance to stress. Major components of the LPS molecule include O-antigen, outer core, inner core, and lipid A. LPS alterations can increase vulnerability to environmental threats (16), and inner core mutations can enhance susceptibility to hydrophobic agents (16–18). Because LPS can also interact with host Toll-like receptor 4 to initiate innate immune responses, it is likely that *K. pneumoniae* LPS plays a complex role in host-pathogen interactions during bacteremia.

To identify factors required for lung dissemination and bloodstream survival, we used previously analyzed and new transposon insertion site sequencing (InSeq) data from a murine model of bacteremic pneumonia. We identified and validated the LPS core biosynthesis gene *gmhB* as involved in the two late phases of bacteremia, but dispensable for initial site fitness in the lung. We also showed that GmhB is a conserved bacterial factor enhancing fitness in blood filtering organs across multiple Gram-negative pathogens.

RESULTS

Transposon insertion site sequencing identifies *K. pneumoniae* GmhB as a bacteremia fitness factor. To identify *K. pneumoniae* factors enhancing dissemination and bloodstream fitness, we used InSeq data collected in previous studies of lung fitness genes in wild-type and Lipocalin-2 deficient mice (*Lcn2*^{-/-}) (10, 11). Because this is an effective model of bacteremic pneumonia (13, 19, 20), we combined previously published

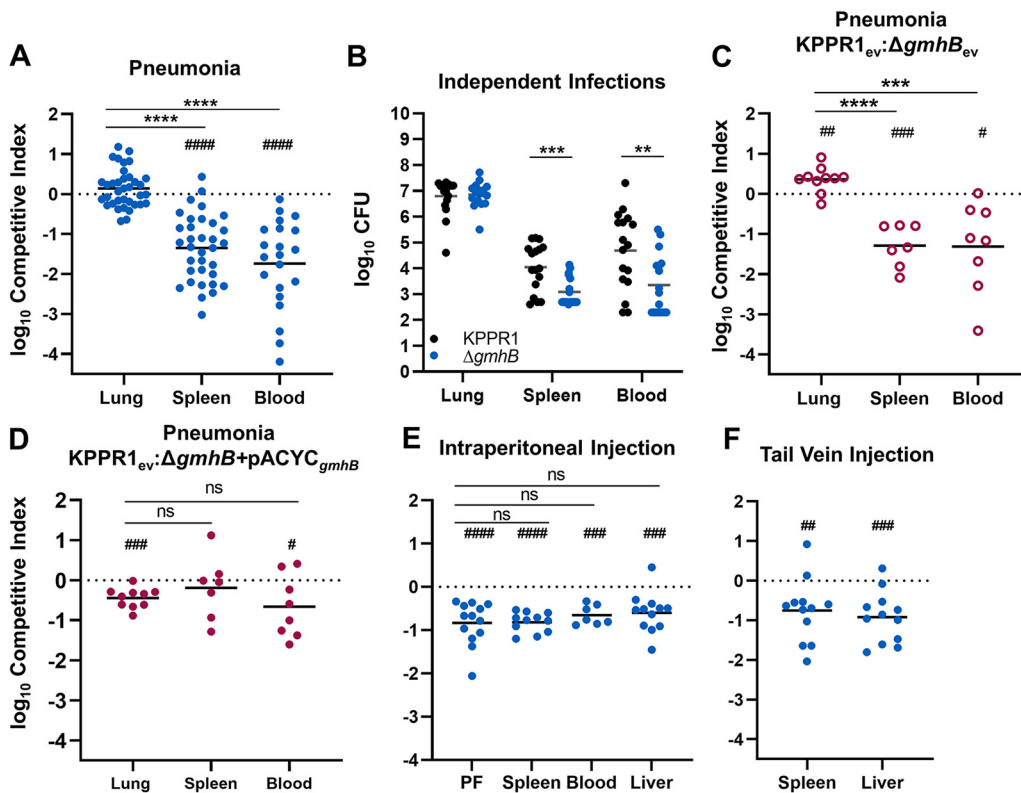


FIG 1 GmhB enhances lung dissemination and bloodstream survival. In a model of bacteremic pneumonia, mice were retropharyngeally inoculated with 1×10^6 CFU *K. pneumoniae* (A to D). To initiate dissemination from a lung-independent site, 1×10^3 CFU was administered to the intraperitoneal cavity (E). For modeling direct bacteremia requiring no dissemination, 1×10^5 CFU was administered via tail vein injection (F). The 1:1 inoculum consisted of KPPR1: $\Delta gmhB$ (A, E, F), KPPR1: $\Delta gmhB$ carrying empty pACYC vector (ev; C), or KPPR1: $\Delta gmhB$ with *gmhB* complementation provided on pACYC under the control of the native *gmhB* promoter ($\Delta gmhB$ +pACYC_{*gmhB*}; D). Independent infections used either KPPR1 or $\Delta gmhB$ alone at a 1×10^6 CFU dose (B). Mean \log_{10} competitive index or CFU burden at 24-h postinfection is displayed. **, $P < 0.01$; ***, $P < 0.001$; ****, $P < 0.0001$ by unpaired *t* test; #, $P < 0.01$; ###, $P < 0.001$; ####, $P < 0.0001$ by one sample *t* test with a hypothetical value of zero. For each group, $n \geq 7$ mice in at least two independent infections. PF, peritoneal fluid.

lung InSeq data with a new analysis of archived data from the spleens of these mice. There was a significant bottleneck in dissemination from the lung to spleen in wild-type mice, precluding InSeq analysis of these samples, so the InSeq was performed on spleens from *Lcn2*^{-/-} mice (Fig. S1). Genes were defined as dispensable for lung fitness by similar recovery of transposon insertions between the inoculum and lungs of both genotypes. Genes were identified as enhancing dissemination or splenic fitness by significant differences in recovered CFU between the *Lcn2*^{-/-} lung and spleen (21) (Data set S1). Of the 18 genes identified with this selection (Table S1), six genes with known annotated functions were selected for validation by generating isogenic knockouts of open reading frames using Lambda Red mutagenesis (22). None of the six encoded factors were required for *K. pneumoniae* *in vitro* replication or fitness, defined by similar growth rates and the ability to compete with wild-type KPPR1 in rich Luria-Bertani (LB) and minimal (M9+Glucose) media (Fig. S2). Because the screen was performed in *Lcn2*^{-/-} mice, we used this lineage only to verify our selection approach. Only one factor, GmhB, validated *in vivo* (Fig. S3) and the selection process was concluded to have yielded numerous false positives, likely because the original InSeq experiments were not designed to accommodate for dissemination bottlenecks. Therefore, GmhB was analyzed for contributions to bacteremia pathogenesis.

Multiple models of murine bacteremia support that GmhB enhances bloodstream fitness. To characterize the fitness defect of a *gmhB* mutant, competitive infections were performed in wild-type C57BL/6 mice. The $\Delta gmhB$ mutant had no fitness defect in the lungs of mice after coinfections with KPPR1 (Fig. 1A; Fig. S4A). In contrast,

the *gmhB* mutant had a 24-fold mean fitness defect in the spleen and 104-fold defect in blood. Like coinfections, in independent infections the *gmhB* mutant had no defect in the lung but significant defects in the spleen and blood of infected mice (Fig. 1B). To confirm that this fitness defect was attributable to disruption of *gmhB*, the mutant was complemented in *trans*. The empty plasmid vector had no effect on the results of competitive infections (Fig. 1C). Plasmid carriage had slight effects on lung fitness, with $\Delta gmhB$ carrying the empty vector having slightly higher fitness, and $\Delta gmhB$ with the complementing plasmid having slightly lower fitness, in the lung (Fig. 1C, D; Fig. S4B, C). In contrast, $\Delta gmhB$ with the empty vector was significantly defective for survival in the spleen and blood with plasmid derived *gmhB* complementation ameliorating this defect in the spleen and partially in the blood (Fig. 1D). Combined, these results indicate that GmhB is necessary for lung dissemination, bloodstream survival, or both stages of bacteremia.

To determine if GmhB enhances dissemination from the lung specifically, a bacteremia model involving an independent initial site was used. A KPPR1 and $\Delta gmhB$ coinfection was performed by intraperitoneal injection and competitive indices were calculated after 24 h (Fig. 1E; Fig. S4D). Unlike the lung model, the *gmhB* mutant was defective in initial site fitness within the peritoneal cavity and a similar fitness defect was observed in the spleen, liver, and blood. Therefore, GmhB influences initial phase fitness in a site-specific manner. This initial site defect in the intraperitoneal model may mask defects in bloodstream survival. To measure fitness in the third phase of bacteremia, a tail vein injection model was used that bypasses the initial site and dissemination steps. Based on coinfections using a tail vein injection with competitive indices calculated after 24 h (Fig. 1F; Fig. S4E), the *gmhB* mutant had a significant fitness defect in both the spleen and liver. Considering the data across three distinct models of bacteremia, GmhB is consistently necessary for survival in the spleen and liver. It is dispensable for initial site infection in the lung but important in the peritoneal cavity, suggesting site-specific fitness. The contribution of GmhB to the third phase of bacteremia may explain the strong defect in dissemination observed in pneumonia model, but we cannot rule out a specific contribution for egress from the lung.

GmhB does not modulate lung inflammation elicited by *K. pneumoniae* during pneumonia. GmhB is a D,D-heptose 1,7-bisphosphate phosphatase involved in biosynthesis of ADP-heptose (23–25), which is a structural component of the LPS core. ADP-heptose is synthesized through a five-part enzymatic cascade modifying the precursor sedoheptulose 7-phosphate. GmhB is the third enzyme in this reaction, serving to dephosphorylate D-glycero- β -D-manno-heptose 1,7-bisphosphate (HBP) to produce d-glycero- β -D-manno-heptose 1-monophosphate (HMP1) (24). Perhaps because LPS is a conserved virulence factor in Gram-negative bacteria, ADP-heptose is also a soluble proinflammatory mediator (26). Soluble ADP-heptose can be recognized by the host cytosolic receptor alpha kinase 1 (ALPK1) (26), resulting in the formation of TIFAsomes, upregulation of NF- κ b signaling, and inflammatory influx (27–30). We have previously observed that lung inflammation contributes to dissemination of *K. pneumoniae* from the lung to the bloodstream (12, 31). If lung dissemination is GmhB-dependent, then perhaps *K. pneumoniae* relies on soluble ADP-heptose to induce an immune response during pneumonia that enables egress from the lungs.

To measure the contribution of GmhB to lung inflammation, KPPR1 and $\Delta gmhB$ were used in the murine pneumonia model and lung homogenates were surveyed for immune cell recruitment and cytokine activation associated with ADP-heptose signaling (30). As expected, neutrophils and monocytes were the most prominent cell types recruited to the lung during *K. pneumoniae* infection (Fig. 2A; Fig. S5) (32–34). Monocytic-myeloid derived suppressor cells (M-MDSCs), which alter the lung immune environment during *K. pneumoniae* infection (35, 36), were decreased after infection, but not in a GmhB-dependent manner. Alveolar macrophages, eosinophils, and dendritic cells were detected by flow cytometry but the abundance of these cell types was not altered by *K. pneumoniae* infection. Importantly, GmhB did not influence the overall CD45⁺ cell abundance in the lung during pneumonia, nor did GmhB alter the profile of any prominent immune cell subset after infection (Fig. 2A). We also measured the abundance of TNF- α ,

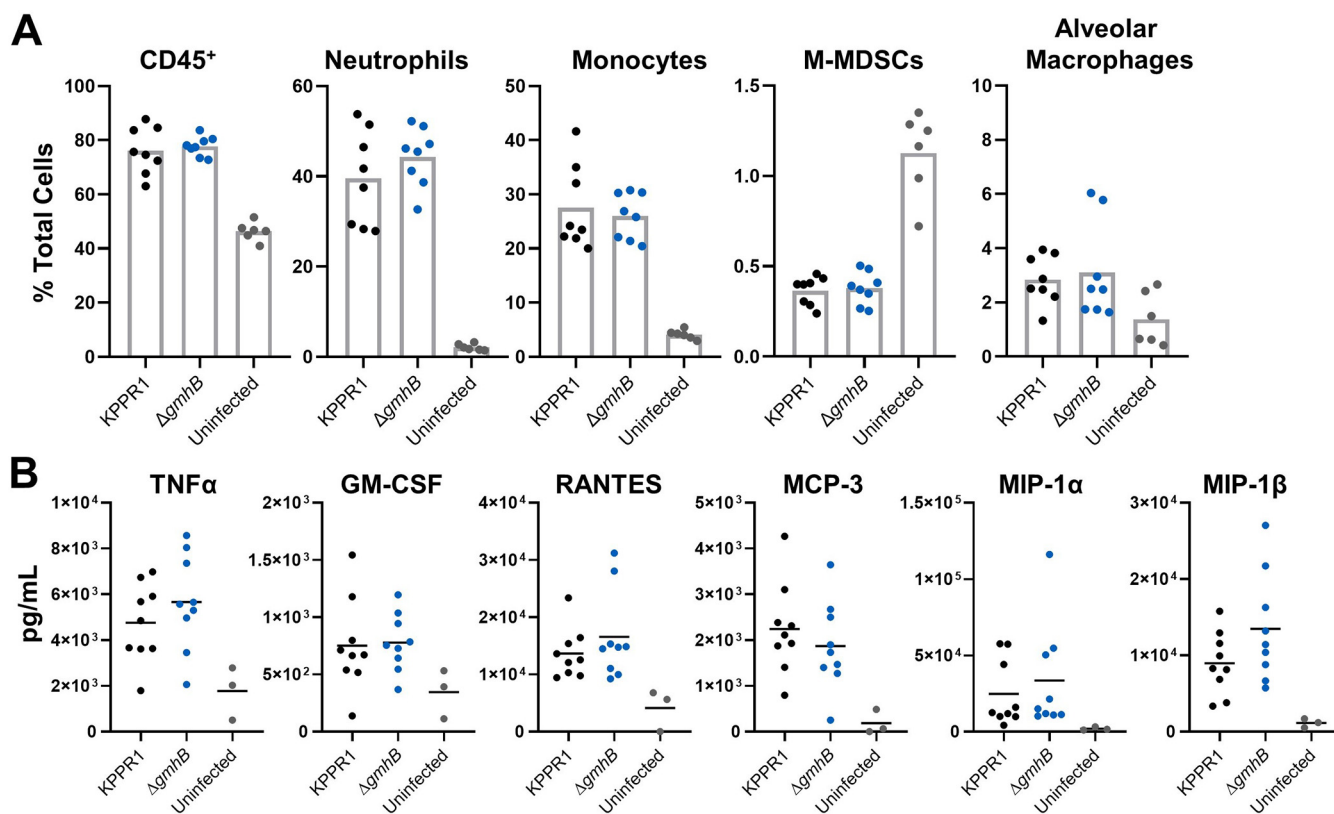


FIG 2 GmhB does not alter normal immune responses during *K. pneumoniae* lung infection. In a model of bacteremic pneumonia, mice were retropharyngeally inoculated with 1×10^6 CFU of either KPPR1 or Δ gmhB. After 24 h, lungs were prepared for flow cytometry using 1.5×10^6 cells/lung. Comparisons between immune cell populations for KPPR1 or Δ gmhB infected or uninfected mice are displayed for relevant subsets (A). Cytokines associated with ADP-heptose/ALPK1 signaling were detected from lung homogenates using ELISA (B). For each infected group, $n = 8$ to 9 mice, and for each uninfected group, $n = 3$ to 6. Each panel represents infections from at least two independent experiments; no comparisons were significant by unpaired *t* test between KPPR1 and Δ gmhB.

GM-CSF, RANTES, MCP-3, MIP-1 α , and MIP-1 β , which are associated with signaling via the ADP-heptose/ALPK1/NF- κ B axis (30), in lung homogenates. Abundance of each analyte was increased after *K. pneumoniae* infection, yet GmhB did not influence signaling by this axis (Fig. 2B). Therefore, inflammation during *K. pneumoniae* lung infection is not GmhB-dependent, as measured by immune cell recruitment and signaling through ADP-heptose/ALPK1/NF- κ B associated cytokines. The influence of GmhB on dissemination and bloodstream survival is likely independent of lung inflammatory responses.

GmhB enhances bloodstream survival by mediating spleen fitness. Given that GmhB enhanced *K. pneumoniae* bloodstream survival during direct bacteremia (Fig. 1F) and did not alter inflammation in the lungs (Fig. 2), we investigated the direct role that it may play on bacterial fitness. Disruption of GmhB during ADP-heptose biosynthesis can influence LPS structure in *E. coli* (24, 25), and LPS core alterations may enhance serum susceptibility (23, 37). To determine if GmhB conveys resistance to serum killing, KPPR1 and Δ gmhB were exposed to active human and murine serum. An Δ rfaH acapsular mutant was used as a control that is highly susceptible to human serum killing (11). In contrast to RfaH, GmhB was dispensable for resistance to human serum-mediated killing (Fig. 3A). Unlike human serum, murine serum was unable to elicit killing in any strain and may lack the ability to form an active membrane attack complex against *K. pneumoniae* (Fig. 3B), a phenomenon observed in other Gram-negative species (38). Additionally, GmhB was not required for growth in active human serum (Fig. 3C). To rule out subtle differences in fitness in human serum, competitive survival assays were performed in human serum. This also showed no defect of the *gmhB* mutant (Fig. 3D; Fig. S6). Thus, the bloodstream survival advantage conveyed by GmhB is likely independent of the ability to resist complement-mediated killing or to replicate in serum.

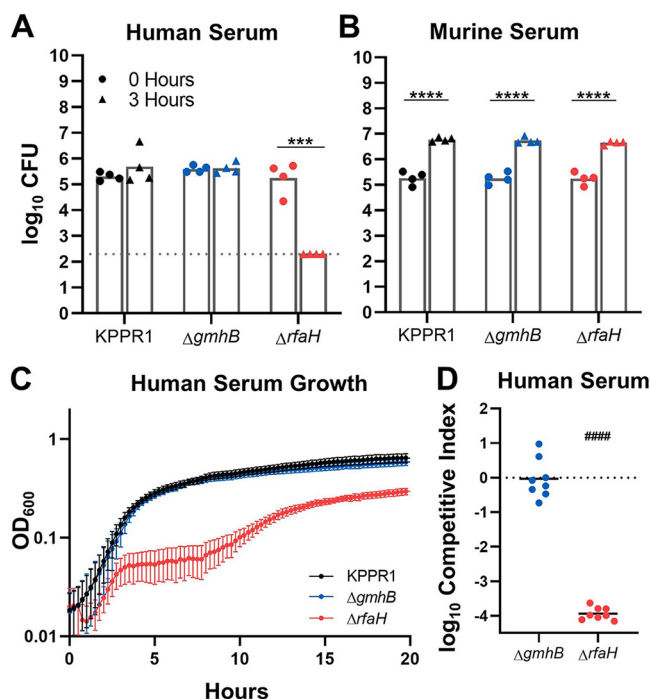


FIG 3 Bloodstream fitness conveyed by GmhB is serum independent. Serum susceptibility was compared after 3 h for 1×10^5 CFU KPPR1, $\Delta gmhB$, and $\Delta rfaH$ in active human (A) or murine (B) serum. *K. pneumoniae* strains were grown in M9 + 20% active human serum and the OD₆₀₀ was measured every 15 min for 20 h (C). Competition assays were performed *in vitro* using active human serum (D) using a 1:1 mixture of 1×10^5 KPPR1 and either $\Delta gmhB$ or $\Delta rfaH$. Mean log₁₀ competitive index compared to wild-type KPPR1 at 3-h postinfection is displayed. ***, $P < 0.001$; ****, $P < 0.0001$ by unpaired *t* test with $n = 4$ (A to B) and limit of detection is represented by the dotted line. For D, $P < 0.0001$ by one sample *t* test with a hypothetical value of zero and $n = 8$.

During bacteremia, *Klebsiella* pass through blood filtering organs, such as the liver and spleen, and GmhB conveyed a fitness advantage in these organs *in vivo* (Fig. 1F). Because the fitness defects of $\Delta gmhB$ during bacteremia are not explained by fitness in serum, we performed *ex vivo* competition assays in uninfected murine spleen and liver homogenates. GmhB was necessary for complete fitness in spleen homogenate (Fig. 4A; Fig. S6). Further, the magnitude of GmhB fitness loss in *ex vivo* spleen homogenate was similar to that observed *in vivo* using tail vein injections (Fig. 1F). RfaH was dispensable for spleen homogenate fitness (Fig. 4A) suggesting that capsule is not required for splenic survival. Furthermore, GmhB was dispensable for hypermucoviscosity (39) (Fig. S7). Despite finding a fitness defect and fewer $\Delta gmhB$ CFU in the liver during infection (Fig. 1E, F and Fig. S4D, S4E), GmhB was dispensable for liver fitness *ex vivo* (Fig. 4B). Similar to its neutral fitness in the lung, the *gmhB* mutant had no defect in lung homogenate *ex vivo* (Fig. 4C). These data indicate that GmhB contributes to bacteremia fitness during the phase of bloodstream survival through spleen-specific interactions.

GmhB is required for normal *K. pneumoniae* LPS composition. GmhB contributes to LPS structure through synthesis of ADP-heptose, a major component of the inner core region. In *E. coli*, GmhB is required for normal LPS composition; GmhB-deficient strains produce a mixed phenotype of full-length and stunted LPS molecules (25). This partial defect is attributed to an uncharacterized enzyme that is partially redundant for GmhB function. In other species, disruption of ADP-heptose integration into LPS results in stunted molecules with minimal O-antigen (17, 18). To determine the impact of *gmhB* deletion on *K. pneumoniae* surface structure, LPS from KPPR1, $\Delta gmhB$, and $\Delta gmhB + pACYC_{gmhB}$ was isolated and analyzed using electrophoresis. Wild-type KPPR1 LPS produces prominent O-antigen laddering patterns similar to the pattern of the *E. coli* LPS standard (Fig. 5). The *K.*

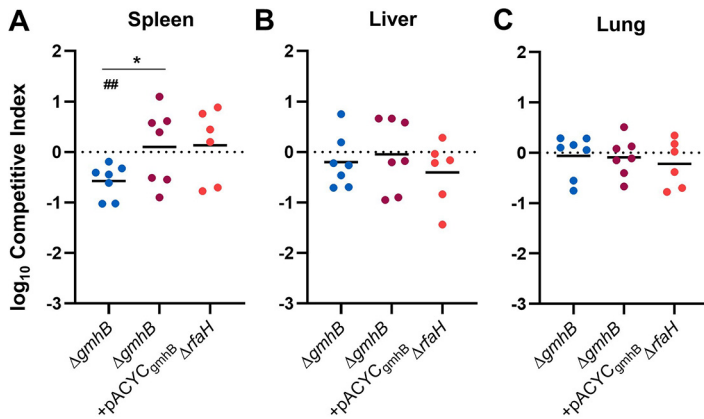


FIG 4 Bloodstream fitness conveyed by GmhB involves interactions in the spleen. Competition assays were performed *ex vivo* in murine spleen (A), liver (B), or lung (C) homogenate using a 1:1 mixture of 1×10^5 KPPR1 and either $\Delta gmhB$, $\Delta gmhB + pACYC_{gmhB}$ or $\Delta rfaH$. Mean \log_{10} competitive index compared to wild-type KPPR1 at 3 h postinoculation is displayed. *, $P < 0.05$, by unpaired *t* test comparing $\Delta gmhB$ and $\Delta gmhB + pACYC_{gmhB}$. ## <0.01 , by one sample *t* test with a hypothetical value of zero and $n = 6$ to 7.

pneumoniae strain $\Delta galU$ (39, 40) lacks prominent O-antigen and can be used to identify regions corresponding to core polysaccharides. In three prominent core banding regions, differences were observed between wild-type KPPR1 and $\Delta gmhB$. Specifically, there was decreased band intensity in heavier bands (regions A and B) and the appearance of banding in region C. These changes were reversed upon *gmhB* complementation. This result indicates that GmhB is required for normal *K. pneumoniae* LPS structure. Similar to *E. coli*, GmhB is not absolutely required for LPS synthesis as O-antigen laddering is still detected even in the absence of this enzyme.

GmhB is a conserved bacteremia fitness factor across multiple clinically relevant Gram-negative pathogens. GmhB is highly conserved across *Enterobacteriales*, which compose the majority of Gram-negative bacteremia pathogens. To address the requirement of GmhB in bloodstream fitness across multiple species, tail vein injections were performed using a coinfection of wild type *E. coli* CFT073 or *C. freundii* UMH14

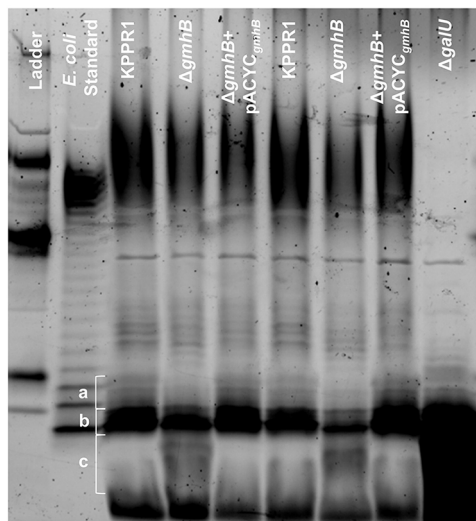


FIG 5 GmhB is required for normal LPS composition. LPS from 1×10^9 CFU of KPPR1, $\Delta gmhB$, $\Delta gmhB + pACYC_{gmhB}$ or $\Delta galU$ was isolated and $10 \mu L$ of yield was analyzed by polyacrylamide electrophoresis. LPS core regions in interest are labeled in a, b, and c. The gel displayed is representative of three independent trials, duplicate lanes represent independent LPS preparations. The CandyCane glycoprotein molecular weight standard is displayed in the left lane.

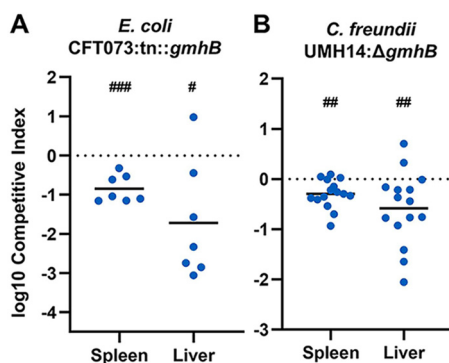


FIG 6 GmhB is required for bacteremia fitness across multiple Gram-negative species. In a model of bacteremia, 1×10^7 CFU of *E. coli* CFT073 (A) or 7.5×10^7 CFU *C. freundii* UMH14 (B) was administered via tail vein injection. The 1:1 inoculum consisted of CFT073:tn::gmhB (A) or 1:2 inoculum of UMH14:ΔgmhB (B). Mean log₁₀ competitive index or CFU burden at 24 h postinfection is displayed. #, $P < 0.05$; ##, $P < 0.01$; ###, $P < 0.001$ by one sample *t* test with a hypothetical value of zero. For each group, $n \geq 7$ mice in at least two independent infections.

and corresponding *gmhB* mutants CFT073:tn::gmhB (41) and UMH14Δ*gmhB*, respectively. GmhB was required for bloodstream survival in both *E. coli* and *C. freundii* as measured in the spleen and liver (Fig. 6; Fig. S8). Additionally, GmhB is a predicted essential gene for *S. marcescens* survival (42). These results reveal that GmhB is a conserved factor enhancing fitness in blood filtering organs across multiple clinically relevant Gram-negative bacteremia pathogens.

DISCUSSION

During bacteremia, *K. pneumoniae* virulence and fitness factors may act during (i) initial site invasion, (ii) dissemination, and (iii) bloodstream survival (3). Based on data from multiple infection models, we identified GmhB as important in the third phase of bacteremia: bloodstream survival. In a model of bacteremic pneumonia, GmhB was dispensable for lung fitness but enhanced fitness in the spleen. In *ex vivo* growth assays, GmhB was specifically important for spleen fitness. Furthermore, GmhB was also required by *E. coli* and *C. freundii* for enhanced fitness in blood-filtering organs. Overall, this study indicates that GmhB is a conserved Gram-negative bacteremia fitness factor.

Distinguishing the three pathogenesis phases of Gram-negative bacteremia can be difficult using *in vivo* infection models. While bacteremic pneumonia modeling indicated a role for GmhB in the latter two phases of bacteremia (Fig. 1A), dissemination and bloodstream survival are difficult to separate experimentally since these processes occur simultaneously. To probe late phases individually, a dissemination independent model of direct bacteremia was utilized and confirmed a role for GmhB during bloodstream survival (Fig. 1F). However, we cannot rule out a specific role in dissemination. Indeed, the greater Δ*gmhB* fitness defect observed in spleen and blood during bacteremic pneumonia compared to direct bacteremia suggests a role for GmhB in both dissemination and survival (Fig. 1A, F). Lung dissemination mechanisms for *Pseudomonas aeruginosa* have been described and rely on exotoxins and the type 3 secretion system for killing host cells to gain bloodstream access (43–45). *K. pneumoniae* does not encode these factors (46). Instead, lung dissemination in *Klebsiella* requires a different host-pathogen interaction, where *K. pneumoniae* siderophores activate epithelial HIF-1α that is in turn required for dissemination (12). The precise mechanism of, and additional factors required for, dissemination from the lung is unclear.

GmhB is involved in the biosynthesis of ADP-heptose, a metabolite detected in host cytosol that initiates inflammation through the ALPK1/TIFA/NF-κB axis (27–30, 47, 48). GmhB dephosphorylates HBP to yield HMP1, which is converted into ADP-heptose. In the present study, GmhB was dispensable for normal inflammation during pneumonia as determined by immune cell recruitment and cytokines signatures associated with

ALPK1/TIFA/NF- κ B signaling. Therefore, lung inflammation elicited by *K. pneumoniae* may not require ADP-heptose or may be activated by other *K. pneumoniae* PAMPs. The minor differences in the LPS electrophoresis pattern in the absence of GmhB indicates that, as in *E. coli* (24, 30), *K. pneumoniae* possesses an unknown mechanism with partially redundant GmhB function (Fig. 5). In the absence of GmhB, this mechanism may produce sufficient ADP-heptose to induce inflammation via the ALPK1/TIFA/NF- κ B axis, leading to normal inflammation observed in Fig. 2.

K. pneumoniae LPS O-antigen is required for serum resistance (14), but its role in lung fitness may vary. The strain KPPR1 requires LPS O-antigen for initial site lung fitness, while it is dispensable for the strain 5215R (13, 49). In *Salmonella typhimurium*, complete abrogation of ADP-heptose integration into LPS results in a molecule lacking core and O-antigen (17, 18) and displays a rough phenotype. Here, GmhB was required for normal LPS biosynthesis but was not absolutely required for production of full-length LPS containing O-antigen. Additionally, KPPR1 retained high levels of hypermucoviscosity in the absence of GmhB. Therefore, GmhB appears to maximize ADP-heptose biosynthesis and contribute to wild-type levels of LPS inner core production. Future work should discern how individual components of the LPS molecule contribute to bloodstream fitness and pathogenicity.

GmhB may be crucial under conditions where rapid LPS production is necessary. During murine bacteremia, *K. pneumoniae* exhibits exponential replication in the spleen at 24 h (50). Rapid replication requires substantial LPS export and, in the absence of GmhB, lower abundance of normal LPS may be produced. This may leave Gram-negative species more susceptible to killing by host defenses, such as phagocytosis by immune cells. Our data supports differential requirements of capsule and LPS in site-specific fitness. The requirement of GmhB for fitness in the spleen *in vivo* and *ex vivo*, but dispensability for human serum resistance and lung and liver fitness *in vivo* and *ex vivo*, indicates that site specific immune cells like splenic macrophages may be required for *K. pneumoniae* clearance during bacteremia. In contrast, RfaH, necessary for capsule production and hypermucoviscosity, is dispensable for *ex vivo* spleen, liver, and lung fitness but required for human serum resistance and *in vivo* lung fitness (11). This suggests that there are distinct interactions between *Klebsiella* and host defenses at each site of infection that require different *Klebsiella* virulence factors.

This study is limited by the validation rate of the InSeq selection process. Each InSeq model requires consideration of experimental bottlenecks to assess the maximum transposon library complexity which can be utilized (51, 52). Only one of the six hits chosen for validation significantly impacted bacteremia pathogenesis, suggesting that stochastic loss from a bottleneck generated a high rate of false positive hits. In future studies, this bottleneck could be mitigated by splitting the transposon library into smaller pools and increasing the number of replicates for each pool.

GmhB is a conserved fitness factor across multiple species that cause bacteremia. Here, we confirmed a role for GmhB in enhancing fitness in blood-filtering organs for *K. pneumoniae*, *E. coli*, and *C. freundii*. InSeq analysis of *C. freundii* bacteremia fitness factors also indicated a role for GmhB in bloodstream fitness (53). Whereas GmhB is conditionally essential in these species, in *S. marcescens*, GmhB appears to be essential for growth (42). This consistent requirement for bloodstream survival makes GmhB and core LPS synthesis pathways attractive candidates for novel therapeutics to treat bacteremia.

MATERIALS AND METHODS

Transposon InSeq. Construction of the *K. pneumoniae* transposon library using the pSAM_Cam plasmid and InSeq analysis was described previously (11). Briefly, after infection with the *K. pneumoniae* transposon library, CFU from total organ homogenate were recovered. DNA from recovered transposon mutants was extracted and fragments were prepared for Illumina sequencing using previously detailed methods (54). To identify lung dissemination and bloodstream survival factors, we devised a stepwise approach using InSeq data from the spleens of *Lcn2*^{-/-} mice and eliminated genes with fitness defects in the lung or interactions with Lipocalin 2: Genes containing transposon insertions were compared between the inoculum, *Lcn2*^{+/+} lung, *Lcn2*^{-/-} lung, and *Lcn2*^{-/-} spleen output pools. Of the 3,707

mutated genes shared across the input and each output pool, 1,489 contained four or more unique transposon insertions (i.e., median number of unique insertions per gene) and were used for subsequent selection steps. To eliminate genes influencing lung fitness, transposon mutants with similar abundance ($q > 0.05$) between the inoculum and *Lcn2*^{+/+} mouse lungs were retained. To eliminate genes that interact with Lipocalin 2 in the lungs, only transposon mutants with similar recovery ($q > 0.05$) between the *Lcn2*^{+/+} and *Lcn2*^{-/-} lung output pools were retained. To identify factors involved in either the phase of lung egress or bloodstream survival, transposon mutants were selected with a significant difference in abundance between the *Lcn2*^{-/-} lung and *Lcn2*^{-/-} spleen output pools ($q < 0.05$). This InSeq selection process resulted in 18 genes with transposon insertions (Table S1) as candidates for encoding dissemination and bloodstream survival factors. All transposon sequencing files are available from the NCBI SRA database (PRJNA270801).

Bacterial strains and media. Reagents were sourced from Sigma-Aldrich (St. Louis, MO) unless otherwise noted. *K. pneumoniae* strains were cultured overnight in LB (Fisher Bioreagents, Ottawa, ON) broth at 37°C shaking or grown on LB agar (Fisher Bioreagents) plates at 30°C. *E. coli* CFT073 (55) and *C. freundii* UMH14 (53) strains were cultured overnight in LB broth shaking or grown on LB agar plates at 37°C. Media for isogenic knockout strains and transposon mutants was supplemented with 40 µg/mL kanamycin and pACYC was selected with 50 µg/mL chloramphenicol.

Bacterial strains and plasmids used in this study are detailed in Table S2. Isogenic knockouts were constructed using Lambda Red mutagenesis and electrocompetent KPPR1 as previously described (11, 22). In short, electrocompetent *K. pneumoniae* carrying the pKD46 plasmid was prepared by an overnight culture at 30°C and diluted the following day 1:50 in LB broth containing 50 µg/mL spectinomycin, 50 mM L-arabinose, 0.5 mM EDTA (Promega, Madison, WI), and 10 µM salicylic acid until reaching exponential phase, defined by an OD₆₀₀ of 0.5 to 0.6. Bacterial cells were cooled on ice for 30 min, followed by centrifugation at 8,000 × *g* for 15 min at 4°C. Pellets were washed serially with 50 mL of 1 mM HEPES pH 7.4 (Gibco, Grand Island, NY), 50 mL diH₂O, and 20 mL 10% glycerol before making a final resuspension at 2 to 3 × 10¹⁰ in 10% glycerol. To generate gene-specific target site fragments for Lambda Red mutagenesis, a kanamycin resistance cassette was amplified from the pKD4 plasmid with primers also containing 65 bp regions of homology to the chromosome flanking the *gmhB* open reading frame. The fragment was electroporated into competent KPPR1 containing pKD46 plasmid and transformants were selected on LB agar containing kanamycin after overnight incubation at 37°C. All KPPR1 isogenic knockouts were confirmed by colony PCR using gene internal and flanking primers. The *C. freundii* UMH14:Δ*gmhB* strain was constructed using Lambda Red mutagenesis as follows: Electrocompetent *C. freundii* UMH14 maintaining the pSIM18 recombination plasmid were prepared by harvesting exponentially growing cells cultured in YENB media supplemented with 200 µg/mL hygromycin grown at 30°C with aeration. To induce expression of pSIM18, the temperature was shifted to 42°C for 20 min and then the culture pelleted at 5,000 × *g* for 10 min at 4°C. Cells were washed twice in cold 10% glycerol and resuspended in 100 µL cold 10% glycerol before storage at -80°C. A gene-specific kanamycin resistance cassette was amplified from the pKD4 plasmid using primers containing 40 bp regions of homology to the chromosome flanking the UMH14 *gmhB* open reading frame. This fragment was electroporated into UMH14 pSIM18 electrocompetent cells which were then recovered in LB media for 1 h at 37°C and plated on LB agar containing kanamycin and incubated at 37°C overnight. UMH14:Δ*gmhB* was confirmed by Sanger sequencing and curing of the pSIM18 recombineering plasmid was confirmed by a restoration of hygromycin sensitivity. The primers used in this study are detailed in Table S3.

The KPPR1 *gmhB* complementation plasmid, pACYC_{*gmhB*}, was generated by two fragment Gibson assembly using NEBuilder HiFi DNA Assembly Master Mix (New England Biolabs, Ipswich, MA). The plasmid pACYC184 (pACYC_{ev}; empty vector) was linearized by BamHI and HindIII (New England Biolabs). The *gmhB* locus, including a 500-bp region upstream of the open reading frame was amplified by PCR from KPPR1 (GCF_000755605.1, nucleotides 2,380,173 to 2,379,086) with primers containing homology to linearized pACYC_{ev} described above. The plasmid and *gmhB* containing PCR product were mixed in a 1:2 ratio and Gibson assembly was performed following the manufacturer's protocol. The resulting Gibson product was electroporated and maintained in *E. coli* TOP10 cells (New England Biolabs) and the final construct (pACYC_{*gmhB*}) was confirmed using Sanger sequencing. pACYC_{*gmhB*} and pACYC_{ev} were mobilized into KPPR1 and Δ*gmhB* by electroporation and plasmids were maintained in the presence 50 µg/mL chloramphenicol.

Murine bacteremia models. This study was performed using 6- to 10-week-old C57BL/6 mice (Jackson Laboratory, Bar Harbor, ME) with careful adherence to humane animal handling recommendations (56) and the study was approved by the University of Michigan Institutional Animal Care and Use Committee (protocol: PRO00009406). As a model of bacteremic pneumonia, mice were anesthetized with isoflurane and 1 × 10⁶ CFU *K. pneumoniae* in a 50 µL volume was administered retropharyngeally. For intraperitoneal bacteremia, mice were injected with 1 × 10³ CFU *K. pneumoniae* in a 100 µL volume administered to the peritoneal cavity. For direct bacteremia, mice were injected with 1 × 10⁵ CFU *K. pneumoniae* in a 100 µL volume administered via tail vein injection (57). For all models, overnight LB cultures of *K. pneumoniae* were centrifuged, resuspended, and adjusted to the proper concentration in PBS. Twenty-four hours postinfection, mice were euthanized by carbon dioxide asphyxiation prior to collection of blood, lung, spleen, liver, or peritoneal fluid. Whole blood was collected by cardiac puncture and dispensed into heparin coated tubes (BD, Franklin Lakes, NJ). Peritoneal fluid was collected by dispensing 3 mL PBS into the peritoneal cavity followed by recollection. After collection, all organs were homogenized in PBS. To determine bacterial density, all sites were serially diluted and CFU measured by quantitative plating on LB agar with appropriate antibiotics. To calculate competitive indices, mice were infected with a 1:1 ratio of *K. pneumoniae* wild-type KPPR1 or isogenic mutant strains. Total CFU were determined by LB

agar quantitative plating and mutant strain CFU were quantified by plating on LB agar with appropriate antibiotics. The competitive index was defined as CFU from (mutant output/wild-type output)/(mutant input/wild-type input).

To model *E. coli* bacteremia, mice were inoculated with a 1:1 mixture of CFT073:tn::*gmhB* for a total of 1×10^7 CFU in a 100 μ L volume administered via tail vein injection. To model *C. freundii* bacteremia, UMH14 and UMH14: Δ *gmhB* stationary-phase cultures were back diluted (1:100) into fresh LB media and grown to late exponential phase at 37°C with aeration. These cultures were centrifuged at $5,000 \times g$ for 10 min at 4°C, and the pellets were suspended in cold PBS to 5×10^8 CFU/mL for UMH14 and 1×10^9 CFU/mL for UMH14: Δ *gmhB* and then combined 1:1. 100 μ L of the combined suspension, which constituted a total inoculum of 7.5×10^7 CFU at a 1:2 CFU ratio of wild-type to mutant, was administered by tail vein injection. For *E. coli* and *C. freundii*, enumeration of total CFU per organ was performed with serial dilution plating as above (using 50 μ g/mL kanamycin for *C. freundii*), and the calculation of competitive indices were determined as described above.

Flow cytometry. Lung homogenate was collected 24-h postinfection with either KPPR1 or Δ *gmhB* in the bacteremic pneumonia model. Lungs were prepared for flow cytometry using single cell suspensions as previously described (58). In short, lungs were resected, minced, and digested in a buffer containing complete DMEM (10% FBS), 15 mg/mL collagenase A (Roche, Basel, Switzerland) and 2,000 units of DNase for 30 min at 37°C. Following digestion, samples were disrupted by repeated aspiration through a 10 mL syringe. Leukocytes were isolated by centrifuging disrupted tissue through a 20% Percoll Solution ($2,000 \times g$ for 20 min). 1.5×10^6 leukocytes were stained with diluted antibody for 30 min on ice before analysis on a BD Fortessa Cytometer. Staining antibodies included: BV650-CD11b (clone M1/70), BV421-I-Ab (MHCII clone AF6-120.1), APC-Cy7-SiglecF (clone E50-2440), purchased from BD Horizon; PE-eFluor610-CD11c (clone N418), purchased from eBioscience; BV605-CD62L (clone MEL-14), BV510-Cx3CR1 (clone SA011F11), AlexaFluor700-CD45 (clone I3/2.3), PE-CD64 (clone X54-5/7.1), PerCP-Cy5.5-CD24 (clone M1/69), PE-Cy7-Ly6C (clone HK1.4), BV570-Ly6G (clone 1A8), APC-CD115 (clone AF598), purchased from Biolegend. Visualization of cell populations was assembled using FlowJo (Version 10.7.2).

Cytokine enzyme-linked immunosorbent assay. Mice were infected with either KPPR1 or Δ *gmhB* using the bacteremic pneumonia model and lungs were homogenized with tissue protein extraction reagent (T-PER, Fisher). Homogenate was centrifuged at $500 \times g$ for 5 min and the supernatant was analyzed for cytokine abundance by the University of Michigan Rogel Cancer Center Immunology Core Facility using enzyme-linked immunosorbent assay (ELISA).

Serum killing and growth assays. To measure serum susceptibility, 1×10^5 CFU of stationary-phase *K. pneumoniae* was added to 100% active human (Invitrogen, Waltham, MA) or C57B/L6 murine serum (Invitrogen). Plates were incubated at 37°C for 3 h, and killing was measured by serial dilutions and quantitative culture at $t = 0$ and $t = 3$. To assess growth, overnight LB broth *K. pneumoniae* cultures were adjusted to 1×10^7 CFU/mL in M9 salts plus 20% human serum in a 96-well dish. Samples were incubated at 37°C and OD₆₀₀ readings were measured every 15 min using an Eon microplate reader and Gen5 software (Version 2.0, BioTek, Winooski, VT).

Ex vivo survival assay. Spleen, liver, and lung from uninfected mice were homogenized in 2 mL PBS. Overnight LB broth *K. pneumoniae* cultures were adjusted to 1×10^6 CFU/mL in PBS and mixed 1:1 for competitive growth. From the bacterial suspension, 10 μ L was added to 90 μ L of organ homogenate for a final concentration of 1×10^5 CFU/mL and incubated for 3 h at 37°C. Survival was measured by serial dilutions and quantitative culture at $t = 0$ and $t = 3$.

LPS isolation and electrophoresis. LPS from 1×10^9 CFU of each strain of interest was isolated using the Sigma Lipopolysaccharide isolation kit according to the manufacturer's instructions. Electrophoresis was performed using a 4% to 20% mini-PROTEAN TGX Precast gel (Bio-Rad, Hercules, CA). LPS was visualized by staining with the Pro-Q Emerald 300 Lipopolysaccharide Gel Stain Kit (Molecular Probes, Eugene, OR).

Statistical analysis. Each *in vivo* experiment was performed in at least two independent infections, and each *in vitro* experiment was an independent biological replicate. For each study, statistical significance was defined as a *P*-value <0.05 (GraphPad Software, La Jolla, CA) as determined by one-sample test to assess differences from a hypothetical competitive index of zero, unpaired *t* test to assess differences between two groups, or ANOVA followed by Tukey's multiple comparisons *post hoc* test to assess differences among multiple groups.

SUPPLEMENTAL MATERIAL

Supplemental material is available online only.

SUPPLEMENTAL FILE 1, XLSX file, 0.7 MB.

SUPPLEMENTAL FILE 2, PDF file, 1.4 MB.

ACKNOWLEDGMENTS

C.L.H. is supported by the Lung Immunopathology Training Grant (T32HL007517); S.J.G. is supported by R35HL144481; L.V.U. is supported by the Molecular Mechanisms in Microbial Pathogenesis Training Program (32AI007528-21A1); G.B.S., H.L.T.M., and M.A.B. are supported by AI134731 from the National Institutes of Health.

We thank Mark T. Anderson for technical support in LPS isolation and electrophoresis. All authors disclose no conflicts of interest.

REFERENCES

- Singer M, Deutschman CS, Seymour CW, Shankar-Hari M, Annane D, Bauer M, Bellomo R, Bernard GR, Chiche J-D, Cooper-Smith CM, Hotchkiss RS, Levy MM, Marshall JC, Martin GS, Opal SM, Rubenfeld GD, van der Poll T, Vincent J-L, Angus DC. 2016. The third international consensus definitions for sepsis and septic shock (sepsis-3). *JAMA* 315:801–810. <https://doi.org/10.1001/jama.2016.0287>.
- Diekema DJ, Hsueh P-R, Mendes RE, Pfaller MA, Rolston KV, Sader HS, Jones RN. 2019. The microbiology of bloodstream infection: 20-year trends from the SENTRY antimicrobial surveillance program. *Antimicrob Agents Chemother* 63:e00355-19. <https://doi.org/10.1128/AAC.00355-19>.
- Holmes CL, Anderson MT, Mobley HLT, Bachman MA. 2021. Pathogenesis of Gram-negative bacteremia. *Clin Microbiol Rev* 34. <https://doi.org/10.1128/CMR.00234-20>.
- Martin RM, Cao J, Brisse S, Passet V, Wu W, Zhao L, Malani PN, Rao K, Bachman MA. 2016. Molecular epidemiology of colonizing and infecting isolates of *Klebsiella pneumoniae*. *mSphere* 1:e00261-16. <https://doi.org/10.1128/mSphere.00261-16>.
- Gorrie CL, Mirčeta M, Wick RR, Edwards DJ, Thomson NR, Strugnell RA, Pratt NF, Garlick JS, Watson KM, Pilcher DV, McGloughlin SA, Spelman DW, Jenney AWJ, Holt KE. 2017. Gastrointestinal carriage is a major reservoir of *Klebsiella pneumoniae* infection in intensive care patients. *Clin Infect Dis* 65:208–215. <https://doi.org/10.1093/cid/cix270>.
- Magill SS, Edwards JR, Bamberg W, Beldavs ZG, Dumyati G, Kainer MA, Lynfield R, Maloney M, McAllister-Hollod L, Nadle J, Ray SM, Thompson DL, Wilson LE, Fridkin SK, Emerging Infections Program Healthcare-Associated Infections and Antimicrobial Use Prevalence Survey Team. 2014. Multistate point-prevalence survey of health care-associated infections. *N Engl J Med* 370:1198–1208. <https://doi.org/10.1056/NEJMoa1306801>.
- CDC. 2013. Antibiotic resistance threats in the United States, 2013. U.S. Department of Health and Human Services, Centers for Disease Control and Prevention, Atlanta, GA.
- CDC. 2019. Antibiotic resistance threats in the United States, 2019. U.S. Department of Health and Human Services, Centers for Disease Control and Prevention, Atlanta, GA.
- Ahn D, Bhushan G, McConville TH, Annavajhala MK, Soni RK, Wong Fok Lung T, Hofstaedter CE, Shah SS, Chong AM, Castano VG, Ernst RK, Uhlemann A-C, Prince A. 2021. An acquired acyltransferase promotes *Klebsiella pneumoniae* ST258 respiratory infection. *Cell Rep* 35:109196. <https://doi.org/10.1016/j.celrep.2021.109196>.
- Vornhagen J, Sun Y, Breen P, Forsyth V, Zhao L, Mobley HLT, Bachman MA. 2019. The *Klebsiella pneumoniae* citrate synthase gene, *gltA*, influences site specific fitness during infection. *PLoS Pathog* 15:e1008010. <https://doi.org/10.1371/journal.ppat.1008010>.
- Bachman MA, Breen P, Deornellas V, Mu Q, Zhao L, Wu W, Cavalcoli JD, Mobley HLT. 2015. Genome-wide identification of *klebsiella pneumoniae* fitness genes during lung infection. *mBio* 6:e00775. <https://doi.org/10.1128/mBio.00775-15>.
- Holden VI, Breen P, Houle S, Dozois CM, Bachman MA. 2016. *Klebsiella pneumoniae* Siderophores induce inflammation, bacterial dissemination, and HIF-1 α stabilization during pneumonia. *mBio* 7:e01397-16. <https://doi.org/10.1128/mBio.01397-16>.
- Lawlor MS, Hsu J, Rick PD, Miller VL. 2005. Identification of *Klebsiella pneumoniae* virulence determinants using an intranasal infection model. *Mol Microbiol* 58:1054–1073. <https://doi.org/10.1111/j.1365-2958.2005.04918.x>.
- Short FL, Di Sario G, Reichmann NT, Kleanthous C, Parkhill J, Taylor PW. 2020. Genomic profiling reveals distinct routes to complement resistance in *Klebsiella pneumoniae*. *Infect Immun* 88:e00043-20. <https://doi.org/10.1128/IAI.00043-20>.
- Weber BS, De Jong AM, Guo ABY, Dharavath S, French S, Fiebig-Comyn AA, Coombes BK, Magolan J, Brown ED. 2020. Genetic and chemical screening in human blood serum reveals unique antibacterial targets and compounds against *Klebsiella pneumoniae*. *Cell Rep* 32:107927. <https://doi.org/10.1016/j.celrep.2020.107927>.
- Roantree RJ, Kuo TT, MacPhee DG. 1977. The effect of defined lipopolysaccharide core defects upon antibiotic resistances of *Salmonella typhimurium*. *J Gen Microbiol* 103:223–234. <https://doi.org/10.1099/00221287-103-2-223>.
- Sirisena DM, Brozek KA, MacLachlan PR, Sanderson KE, Raetz CR. 1992. The *rfaC* gene of *Salmonella typhimurium*. Cloning, sequencing, and enzymatic function in heptose transfer to lipopolysaccharide. *J Biol Chem* 267:18874–18884. [https://doi.org/10.1016/S0021-9258\(19\)37042-5](https://doi.org/10.1016/S0021-9258(19)37042-5).
- Sirisena DM, MacLachlan PR, Liu SL, Hessel A, Sanderson KE. 1994. Molecular analysis of the *rfaD* gene, for heptose synthesis, and the *rfaF* gene, for heptose transfer, in lipopolysaccharide synthesis in *Salmonella typhimurium*. *J Bacteriol* 176:2379–2385. <https://doi.org/10.1128/jb.176.8.2379-2385.1994>.
- Bachman MA, Oyler JE, Burns SH, Caza M, Lépine F, Dozois CM, Weiser JN. 2011. *Klebsiella pneumoniae* yersiniabactin promotes respiratory tract infection through evasion of lipocalin 2. *Infect Immun* 79:3309–3316. <https://doi.org/10.1128/IAI.05114-11>.
- Broberg CA, Wu W, Cavalcoli JD, Miller VL, Bachman MA. 2014. Complete genome sequence of *Klebsiella pneumoniae* strain ATCC 43816 KPPR1, a rifampin-resistant mutant commonly used in animal, genetic, and molecular biology studies. *Genome Announc* 2. <https://doi.org/10.1128/genomeA.00924-14>.
- Zhao L, Anderson MT, Wu W, T Mobley HL, Bachman MA. 2017. TnseqDiff: identification of conditionally essential genes in transposon sequencing studies. *BMC Bioinformatics* 18:326. <https://doi.org/10.1186/s12859-017-1745-2>.
- Datsenko KA, Wanner BL. 2000. One-step inactivation of chromosomal genes in *Escherichia coli* K-12 using PCR products. *Proc Natl Acad Sci U S A* 97:6640–6645. <https://doi.org/10.1073/pnas.120163297>.
- García-Weber D, Arriemerlou C. 2021. ADP-heptose: a bacterial PAMP detected by the host sensor ALPK1. *Cell Mol Life Sci* 78:17–29. <https://doi.org/10.1007/s00018-020-03577-w>.
- Kneidinger B, Marolda C, Graninger M, Zamyatina A, McArthur F, Kosma P, Valvano MA, Messner P. 2002. Biosynthesis pathway of ADP-L-glycero-beta-D-manno-heptose in *Escherichia coli*. *J Bacteriol* 184:363–369. <https://doi.org/10.1128/JB.184.2.363-369.2002>.
- Taylor PL, Sugiman-Marangos S, Zhang K, Valvano MA, Wright GD, Junop MS. 2010. Structural and kinetic characterization of the LPS biosynthetic enzyme D-alpha,beta-D-heptose-1,7-bisphosphate phosphatase (GmhB) from *Escherichia coli*. *Biochemistry* 49:1033–1041. <https://doi.org/10.1021/bi901780j>.
- Malott RJ, Keller BO, Gaudet RG, McCaw SE, Lai CCL, Dobson-Belaire WN, Hobbs JL, St Michael F, Cox AD, Moraes TF, Gray-Owen SD. 2013. *Neisseria gonorrhoeae*-derived heptose elicits an innate immune response and drives HIV-1 expression. *Proc Natl Acad Sci U S A* 110:10234–10239. <https://doi.org/10.1073/pnas.1303738110>.
- Milivojevic M, Dangeard A-S, Kasper CA, Tschon T, Emmenlauer M, Pique C, Schnupf P, Guignon J, Arriemerlou C. 2017. ALPK1 controls TIFA/TRAF6-dependent innate immunity against heptose-1,7-bisphosphate of gram-negative bacteria. *PLoS Pathog* 13:e1006224. <https://doi.org/10.1371/journal.ppat.1006224>.
- García-Weber D, Dangeard A-S, Cornil J, Thai L, Rytter H, Zamyatina A, Mulard LA, Arriemerlou C. 2018. ADP-heptose is a newly identified pathogen-associated molecular pattern of *Shigella flexneri*. *EMBO Rep* 19. <https://doi.org/10.15252/embr.201846943>.
- Pfannkuch L, Hurwitz R, Traulsen J, Sigulla J, Poeschke M, Matzner L, Kosma P, Schmid M, Meyer TF. 2019. ADP heptose, a novel pathogen-associated molecular pattern identified in *Helicobacter pylori*. *FASEB J* 33:9087–9099. <https://doi.org/10.1096/fj.201802555R>.
- Zhou P, She Y, Dong N, Li P, He H, Borio A, Wu Q, Lu S, Ding X, Cao Y, Xu Y, Gao W, Dong M, Ding J, Wang D-C, Zamyatina A, Shao F. 2018. Alpha-kinase 1 is a cytosolic innate immune receptor for bacterial ADP-heptose. *Nature* 561:122–126. <https://doi.org/10.1038/s41586-018-0433-3>.
- Bachman MA, Lenio S, Schmidt L, Oyler JE, Weiser JN. 2012. Interaction of lipocalin 2, transferrin, and siderophores determines the replicative niche of *Klebsiella pneumoniae* during pneumonia. *mBio* 3. <https://doi.org/10.1128/mBio.00224-11>.
- Gonzalez-Ferrer S, Peñaloza HF, Budnick JA, Bain WG, Nordstrom HR, Lee JS, Van Tyne D. 2021. Finding order in the chaos: outstanding questions in *Klebsiella pneumoniae* pathogenesis. *Infect Immun* 89. <https://doi.org/10.1128/IAI.00693-20>.

33. Xiong H, Carter RA, Leiner IM, Tang Y-W, Chen L, Kreiswirth BN, Pamer EG. 2015. Distinct contributions of neutrophils and CCR2+ monocytes to pulmonary clearance of different *Klebsiella pneumoniae* strains. *Infect Immun* 83:3418–3427. <https://doi.org/10.1128/IAI.00678-15>.
34. Chen L, Zhang Z, Barletta KE, Burdick MD, Mehrad B. 2013. Heterogeneity of lung mononuclear phagocytes during pneumonia: contribution of chemokine receptors. *Am J Physiol Lung Cell Mol Physiol* 305:L702–L711. <https://doi.org/10.1152/ajplung.00194.2013>.
35. Peñalosa HF, Noguera LP, Ahn D, Vallejos OP, Castellanos RM, Vazquez Y, Salazar-Echegarai FJ, González L, Suazo I, Pardo-Roa C, Salazar GA, Prince A, Bueno SM. 2019. Interleukin-10 produced by myeloid-derived suppressor cells provides protection to carbapenem-resistant *Klebsiella pneumoniae* sequence type 258 by enhancing its clearance in the airways. *Infect Immun* 87. <https://doi.org/10.1128/IAI.00665-18>.
36. Ahn D, Peñalosa H, Wang Z, Wickersham M, Parker D, Patel P, Koller A, Chen El, Bueno SM, Uhlemann A-C, Prince A. 2016. Acquired resistance to innate immune clearance promotes *Klebsiella pneumoniae* ST258 pulmonary infection. *JCI Insight* 1:e89704. <https://doi.org/10.1172/jci.insight.89704>.
37. Xu D, Zhang W, Zhang B, Liao C, Shao Y. 2016. Characterization of a biofilm-forming *Shigella flexneri* phenotype due to deficiency in Hep biosynthesis. *PeerJ* 4:e2178. <https://doi.org/10.7717/peerj.2178>.
38. Siggins MK, Cunningham AF, Marshall JL, Chamberlain JL, Henderson IR, MacLennan CA. 2011. Absent bactericidal activity of mouse serum against invasive African nontyphoidal *Salmonella* results from impaired complement function but not a lack of antibody. *J Immunol* 186:2365–2371. <https://doi.org/10.4049/jimmunol.1000284>.
39. Mike LA, Stark AJ, Forsyth VS, Vornhagen J, Smith SN, Bachman MA, Mobley HLT. 2021. A systematic analysis of hypermucoviscosity and capsule reveals distinct and overlapping genes that impact *Klebsiella pneumoniae* fitness. *PLoS Pathog* 17:e1009376. <https://doi.org/10.1371/journal.ppat.1009376>.
40. Chang HY, Lee JH, Deng WL, Fu TF, Peng HL. 1996. Virulence and outer membrane properties of a *galU* mutant of *Klebsiella pneumoniae* CG43. *Microb Pathog* 20:255–261. <https://doi.org/10.1006/mpat.1996.0024>.
41. Shea AE, Marzoa J, Himpel SD, Smith SN, Zhao L, Tran L, Mobley HLT. 2020. *Escherichia coli* CFT073 fitness factors during urinary tract infection: identification using an ordered transposon library. *Appl Environ Microbiol* 86. <https://doi.org/10.1128/AEM.00691-20>.
42. Anderson MT, Mitchell LA, Zhao L, Mobley HLT. 2017. Capsule production and glucose metabolism dictate fitness during *Serratia marcescens* Bacteremia. *mBio* 8:e00740-17. <https://doi.org/10.1128/mBio.00740-17>.
43. Garrity-Ryan L, Kazmierczak B, Kowal R, Comolli J, Hauser A, Engel JN. 2000. The arginine finger domain of ExoT contributes to actin cytoskeleton disruption and inhibition of internalization of *Pseudomonas aeruginosa* by epithelial cells and macrophages. *Infect Immun* 68:7100–7113. <https://doi.org/10.1128/IAI.68.12.7100-7113.2000>.
44. Shaver CM, Hauser AR. 2004. Relative contributions of *Pseudomonas aeruginosa* ExoU, ExoS, and ExoT to virulence in the lung. *Infect Immun* 72:6969–6977. <https://doi.org/10.1128/IAI.72.12.6969-6977.2004>.
45. Rangel SM, Diaz MH, Knoten CA, Zhang A, Hauser AR. 2015. The role of ExoS in dissemination of *Pseudomonas aeruginosa* during pneumonia. *PLoS Pathog* 11:e1004945. <https://doi.org/10.1371/journal.ppat.1004945>.
46. Paczosa MK, Meecs J. 2016. *Klebsiella pneumoniae*: going on the offense with a strong defense. *Microbiol Mol Biol Rev* 80:629–661. <https://doi.org/10.1128/MMBR.00078-15>.
47. Gaudet RG, Sintsova A, Buckwalter CM, Leung N, Cochrane A, Li J, Cox AD, Moffat J, Gray-Owen SD. 2015. Cytosolic detection of the bacterial metabolite HBP activates TIFA-dependent innate immunity. *Science* 348:1251–1255. <https://doi.org/10.1126/science.aaa4921>.
48. Gall A, Gaudet RG, Gray-Owen SD, Salama NR. 2017. TIFA signaling in gastric epithelial cells initiates the *cag* type 4 secretion system-dependent innate immune response to *Helicobacter pylori* infection. *mBio* 8. <https://doi.org/10.1128/mBio.01168-17>.
49. Cortés G, Borrell N, de Astorza B, Gómez C, Sauleda J, Albertí S. 2002. Molecular analysis of the contribution of the capsular polysaccharide and the lipopolysaccharide O side chain to the virulence of *Klebsiella pneumoniae* in a murine model of pneumonia. *Infect Immun* 70:2583–2590. <https://doi.org/10.1128/IAI.70.5.2583-2590.2002>.
50. Anderson MT, Brown AN, Pirani A, Smith SN, Photenhauer AL, Sun Y, Snitkin ES, Bachman MA, Mobley HLT. 2021. Replication dynamics for six gram-negative bacterial species during bloodstream infection. *mBio* 12:e0111421. <https://doi.org/10.1128/mBio.01114-21>.
51. Abel S, Abel Zur Wiesch P, Davis BM, Waldor MK. 2015. Analysis of bottlenecks in experimental models of infection. *PLoS Pathog* 11:e1004823. <https://doi.org/10.1371/journal.ppat.1004823>.
52. Cain AK, Barquist L, Goodman AL, Paulsen IT, Parkhill J, van Opijnen T. 2020. A decade of advances in transposon-insertion sequencing. *Nat Rev Genet* 21:526–540. <https://doi.org/10.1038/s41576-020-0244-x>.
53. Anderson MT, Mitchell LA, Zhao L, Mobley HLT. 2018. *Citrobacter freundii* fitness during bloodstream infection. *Sci Rep* 8:11792. <https://doi.org/10.1038/s41598-018-30196-0>.
54. Goodman AL, Wu M, Gordon JI. 2011. Identifying microbial fitness determinants by insertion sequencing using genome-wide transposon mutant libraries. *Nat Protoc* 6:1969–1980. <https://doi.org/10.1038/nprot.2011.417>.
55. Mobley HL, Green DM, Trifillis AL, Johnson DE, Chippendale GR, Lockatell CV, Jones BD, Warren JW. 1990. Pyelonephritogenic *Escherichia coli* and killing of cultured human renal proximal tubular epithelial cells: role of hemolysin in some strains. *Infect Immun* 58:1281–1289. <https://doi.org/10.1128/iai.58.5.1281-1289.1990>.
56. (US) NRC. 2011. Guide for the care and use of laboratory animals. National Academies Press, Washington, DC.
57. Smith SN, Hagan EC, Lane MC, Mobley HL. 2010. Dissemination and systemic colonization of uropathogenic *Escherichia coli* in a murine model of bacteremia. *mBio* 1:e00262-10. <https://doi.org/10.1128/mBio.00262-10>.
58. Gurczynski SJ, Pereira NL, Hrycaj SM, Wilke C, Zemans RL, Moore BB. 2021. Stem cell transplantation uncovers TDO-AHR regulation of lung dendritic cells in herpesvirus-induced pathology. *JCI Insight* 6. <https://doi.org/10.1172/jci.insight.139965>.